Design of Highly Efficient Pr^{3+}- doped Chalcogenide Fiber Laser

M A Khamis and K Ennser

Abstract—This letter describes the design of a medium infrared (Mid-IR) laser based on a double clad structure of praseodymium (Pr^{3+})-doped chalcogenide glass. The overlap of the emission cross-sections of Pr^{3+} in the transitions ($^3F_2$, $^3H_6$ → $^3H_5$ and $^3H_5$ → $^3H_4$ enable both transitions to simultaneously produce a single coherent wavelength in the range between 3.7 µm and 4.6 µm. A single pair Fiber Brag Grating (FBG) at the overlapping transition wavelengths is used to avoid fabrication complexity of a cascade pumping scheme. In addition, the proposed design takes advantages of the fact that one excited ion will radiate two photons in the overlapping transition wavelengths. In this paper, the laser performance is tested as a function of fiber length, pump power, signal wavelength, fiber background loss and Pr^{3+} doped concentration. The modeling results reveal that 48% of slope efficiency could be produced when the fiber losses are about 1dB/m.

***Index Terms*— Mid-infrared fiber laser, Praseodymium doped-glass, Chalcogenide glass material.**

I. Introduction

Recently, mid-infrared (MIR) light sources have attracted strong interest for many novel applications, which include environmental monitoring, biomedical sensing, medical diagnostic and homeland security [1-3]. Light sources at this spectral region have many interesting properties include compact, high efficiency, rugged light source [4]. A low phonon energy host material is required to access this spectra region and for this reason chalcogenide glass are promising host material. Chalcogenide glass has high refractive index, good rare earth ion solubility and therefore it is attractive host material for rare earth ions [5,6]. The chalcogenide glass allows light propagation for broad range of wavelengths from 1.5 µm up to 13 µm [7]. The feasibility to achieve high-purity chalcogenide glass and therefore lower fiber loss have increased the interest in MID-IR light source when doped with lanthanides [8]. A theoretical study has shown that Pr^{3+}-doped chalcogenide glass has attractive characteristics in the mid-infrared fluorescence. This is because of high pump absorption cross-section of Pr^{3+} in chalcogenide glass as compare with other lanthanide rare earth ions [9]. Another reason is that Pr^{3+} can be pumped from a commercially available 2 µm diode laser [10]. Additionally, Pr^{3+} have overlapping emission cross-sections in the ($^3F_2$, $^3H_6$) → $^3H_5$ (3.3–4.7 µm), and $^3H_5$→$^3H_4$ (3.7–5.5 µm) transitions [11].

However, there are some problems to realize Pr^{3+}-doped chalcogenide glass fiber laser. One of the issues is the long lifetime of its lower laser level and so it exhibits a poor overall efficiency [12]. A cascade lasing approach is one possible solution to this latter obstacle [13,14]. However, it is required high fabrication complexity which is related to the construction of two pairs of Bragg gratings and two lasing cavities [12]. In addition, it requires a significant pump power in order to achieve laser action for both transitions.

In this letter, we propose a new approach to overcome the difficulties of the population inversion in Pr^{3+}-doped chalcogenide glass fiber laser pumped at 2µm and thanks to Pr^{3+} overlapping emission cross-sections. In this approach, we use a single pair of fiber Bragg gratings which its Bragg wavelength in the wavelength range of the overlapping emission cross-sections (3.7 µm-4.6 µm). One excited ion will be able to emit two photons in Mid-IR range as the same process in cross-relaxation transition of Tm^{+3}doped fiber laser [15]. As a result, more than 48% of power efficiency could be theoretically achieved.

II. Theory and Design

The proposed laser scheme is shown in fig. 1. The pair fiber Bragg gratings (FBG) are tuned for both idler and signal wavelengths with Bragg wavelength at 4500 nm which lies under the overlapping emission cross-sections.

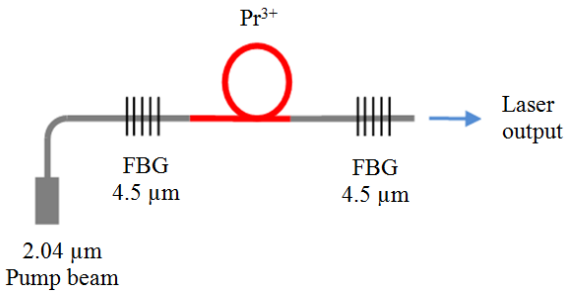

Fig. 1. Schematic diagram of Pr^{3+}- doped chalcogenide fiber laser.

Figure 2 shows the overlap between the two emission cross-sections [9]. They correspond to the emission cross-sections in the ($^3F_2$, $^3H_6$) → $^3H_5$ (3.3–4.7 µm), and $^3H_5$→$^3H_4$ (3.7–5.6 µm)

Submitted on May 31, 2017. This work was supported in part by the European Community MPNS COST Action MP1401 "Advanced fiber laser and coherent source as tools for society, manufacturing and life science."

M. A. Khamis and K. Ennser are with College of Engineering, Swansea University, Swansea, Wales, UK (email: k.ennser@swansea.ac.uk).

transitions. The main ion transitions among the energy levels of Pr^{3+}-doped chalcogenide glass fiber laser is shown in Fig. 3. The typical behavior of the three-level laser system occurs by using a pump beam at the wavelength 2.04 µm.

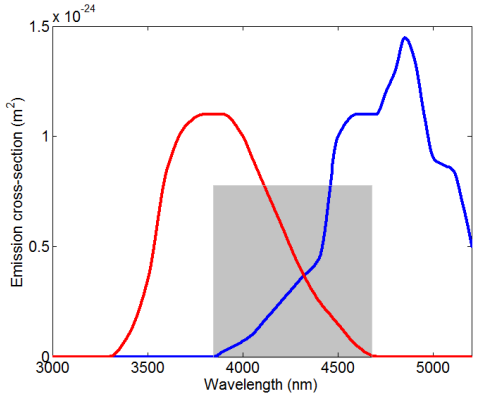

Fig. 2 Emission cross-sections in transition $^3F_2$, $^3H_6 \rightarrow {}^3H_5$ and $^3H_5 \rightarrow {}^3H_4$ [9]. The overlapped emission cross-section is shown in the gray region.

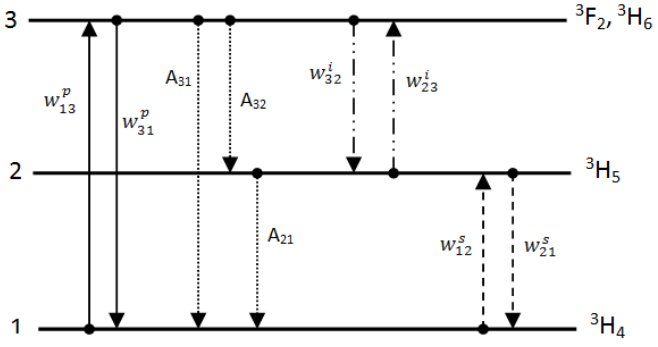

Fig. 3. The three lower energy levels diagram of Pr^{3+}- doped chalcogenide. Note that the pump is at 2.04 µm. Idler and Signal have the same wavelength at 4.5 µm.

The employed model considers the pump absorption and stimulated emission close to the pump wavelength at 2.04 µm and the signal absorption and stimulated emission close to the signal wavelength at 4.5 µm. The laser steady state equations are as follows [16,17]:

$$\begin{bmatrix} C_{11} & C_{12} & C_{13} \\ C_{21} & C_{22} & C_{23} \\ 1 & 1 & 1 \end{bmatrix} \begin{bmatrix} N_1 \\ N_2 \\ N_3 \end{bmatrix} = \begin{bmatrix} 0 \\ 0 \\ N_p \end{bmatrix} \quad (1)$$

The coefficients in Eq.(1) are as follow: $C_{11} = w_{13}^p$, $C_{12} = w_{23}^i$, $C_{13} = -w_{31}^p - w_{32}^i - 1/\tau_3$, $C_{21} = w_{12}^s$, $C_{22} = -w_{21}^s - w_{23}^i - 1/\tau_2$, $C_{23} = w_{32}^i + \beta_{32}/\tau_3$, where τ_3 and τ_2 are the lifetime of level 3 and 2, respectively; β_{32} is the branching ratio of transition of level 3 to 2; The stimulated rates for the pump, signal and idler are given by:

$$w_{ij}^x = \frac{\Gamma_x \sigma_{ij} \lambda_x}{A\, h\, c} \times p_x \quad (2)$$

Where: x=p for pump or s for signal or i for idler, Γ_x is the confinement factor, σ_{ij} is the absorption or emission cross-section for the ij transition, P_x denotes the propagating signal and pump powers, respectively. Note that the idler is the same to signal and under the overlapping transition wavelengths, therefore P_i=P_s. A is the doping cross-section area; h is Planck's constant; c is the speed of light in the free space.

The spatial evolution of the pump and signal powers are obtained by solving the following differential equations:

$$\frac{dP_p^{\pm}}{dz} = \mp\Gamma_p\left[\sigma_{pa}N_1 - \sigma_{pe}N_3\right]P_p^{\pm} \mp \alpha P_p^{\pm} \quad (3)$$

$$\frac{dP_s^{\pm}}{dz} = \mp\Gamma_s[(\sigma_{ia}N_2 - \sigma_{ie}N_3) + (\sigma_{sa}N_1 - \sigma_{se}N_2)]P_s^{\pm} \mp \alpha P_s^{\pm} \quad (4)$$

where '+' and '-' refer to forward and backward travelling which are governing by the following boundary conditions:

$$P_s^+(0) = R_i\, P_s^-(0) \quad (5)$$

$$P_s^-(L) = R_o\, P_s^+(L) \quad (6)$$

Where R_i and R_o are the FBG reflectivity at the input and output of the Pr^{3+}-doped fiber, respectively; L is the laser cavity length. Relaxation algorithm is implemented to solve simultaneously Equations (1)–(4) [13]. We numerically propagated the powers at λ_s back and forth between the mirrors, subject to the reflectivity at the fiber ends. The process is repeated iteratively until a stop condition is fulfilled.

III. Numerical Results

The parameters used in the numerical simulations are taken from [9,17] and shown in Table I. The absorption and emission cross-section at 2.04 µm are shown in fig. 4.

TABLE I
SIMULATION PARAMETERS FOR A P_R^{3+}-DOPED CHALCOGENIDE GLASS FIBRE LASER

Quantity	Value	Unit
Pr^{3+}-ion concentration	5×10^{25}	m^{-3}
Lifetime of level 3	4.2	ms
Lifetime of level 2	12	ms
Branching ratio for 3-2 transitions	0.42	
Pump wavelength	2.04	µm
Signal and Idler wavelength	4.5	µm
Confinement factor for signal and Idler	0.8	
Confinement factor for pump	0.034	
Pump emission cross section	1.4×10^{-24}	m^2
Pump absorption cross section	2.2×10^{-24}	m^2
Idler emission cross section	0.15×10^{-24}	m^2
Idler absorption cross section	0.01×10^{-24}	m^2
Signal emission cross section	0.66×10^{-24}	m^2
Signal absorption cross section	0.75×10^{-24}	m^2

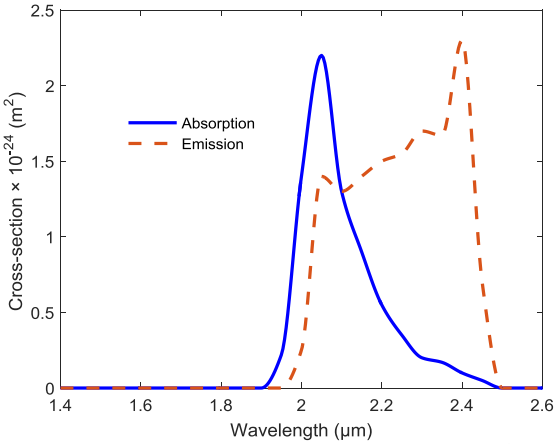

Fig. 4 Absorption and emission cross-sections in transition $^3H_4 \rightarrow {}^3F_2$, $^3H_6$ [17].

For the fiber, we assumed that a conventional double-clad structure with a uniformly doped core radius which guides the signal wavelength in a single-mode. The inner cladding is highly multimode at the pump wavelength. The core radius is 5.5μm, the inner cladding is 30 μm and the numerical aperture is equal to 0.2. The resonator structure of the fiber laser consists pair of fiber Bragg gratings (FBG) to trap the signal. The reflectivity of the input FBG for the pump wavelength is 0.05 and for the signal is 0.95 while the output reflectivity is 0.05 for the signal [9].

Relaxation method is used to solve the differential equations (3) and (4) of the pump and the signal, respectively. We assume the level of losses for the pump and signal wavelengths are 1 dB/m and this value is much higher than the experimentally paper for some chalcogenide glass [12]. Using the data of Table I and the values of the emission and the absorption cross-section spectra [17], we solve numerically the rate equations (1) of the pump model. We investigate the important parameters such as the fiber length, pump power, doping concentration, signal wavelength and fiber losses to evaluate their influence in the laser performance. Firstly, we investigate the influence of laser cavity length. Figure 5 illustrates the laser signal power versus laser cavity length L, for different input pump powers. It can be observed that a reduction in the output power with a further increase in the fiber length. Also, we can see that the output is maximized when laser cavity length equal 1.3 m. In addition, the slope efficiency for 4.5 μm wavelength reaches about 48%. The main limitation factor for getting higher efficiency is the large loss of the chalcogenide host material.

To evaluate our proposed design, we compared our finding with a conventional cascade pumping scheme proposed in [17]. We used two pairs of FBG, one pair is for the idler at 3.7 μm and the other is for the signal at 4.89 μm. The reflectivity of the input and output FBGs for the idler are 0.9 and 0.95, respectively while for the signal are 0.95 and 0.05, respectively. The simulation results in fig. 6 point out the slope efficiency at 4.89 μm wavelength is about 18% and this value is about three times lower than the findings of our proposed design. The reason for the laser efficiency increase in our proposed design is that the idler and signal emission are as same wavelength, so one excited ion can radiate two photons at wavelength 4.5 μm.

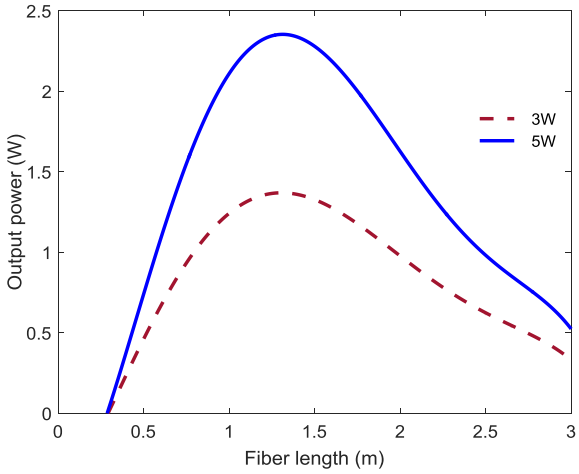

Fig. 5. Laser signal power $P_s(L)$ at 4.5 μm wavelength versus the laser cavity length L, for different input pump powers, $P_p(0)$ = 3 W (red curve), $P_p(0)$ = 5 W (blue curve). Doping concentration $N_p = 5 \times 10^{25}$ ions/m^3; input and output mirror reflectivity R_i = 5% and R_o = 95%.

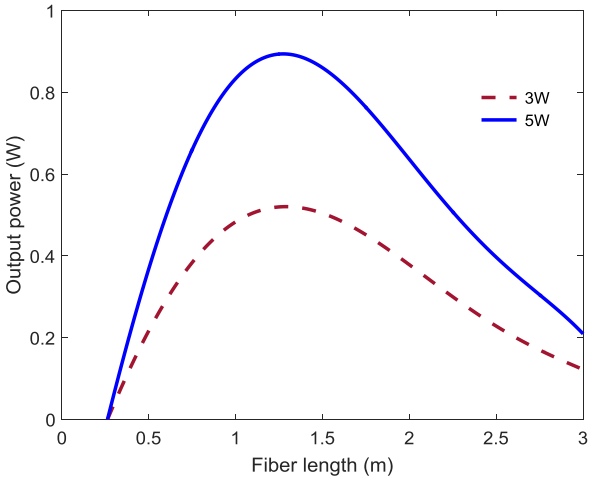

Fig. 6. Laser signal power $P_s(L)$ in a conventional cascade pumping scheme at 4.89 μm wavelength versus laser cavity length L, for different input pump powers, $P_p(0)$ = 3 W (red curve), $P_p(0)$ = 5 W (blue curve). Doping concentration $N_p = 5 \times 10^{25}$ ions/m^3; input and output mirror reflectivity R_i = 5% and R_o = 95% for the signal, 90% and 95% for the idler.

The next investigation is to study the effect of Pr^{3+} doping concentrations on the laser performance. As different doping concentration corresponds to different absorption and emission cross-sections we choose the fiber with 5×10^{25} ions/m^3 described in Table I and another fiber with 2×10^{25} ions/m^3 as described in [5,11]. Note that the other parameters are the same for both fibers. Figure 7 illustrates the dependence of the output laser power on the input pump powers with different Pr^{3+} doping concentrations. In all cases the output lasing wavelength is at 4.5 μm. It is worthwhile noticing that an increase of the output laser power is more apparent for high Pr^{3+} doping concentrations. At concentration 5×10^{25} ions/m^3 there is no signs of crystallization after melt cooling and annealing. However heavily doping concentration might cause glass devitrification [9].

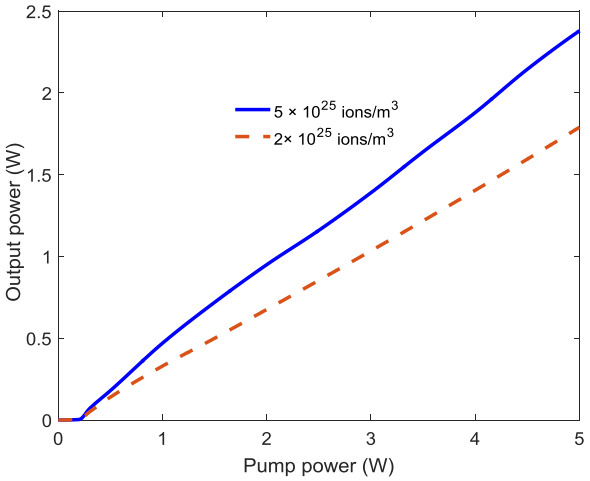

Fig. 7. Calculated output signal power versus the input pump power with different doping concentration.

Figure 8 shows the output laser power as a function of lasing wavelength, for two loss levels, for the pump wavelength and fiber length fixed at 2.04 µm and 1.3 m, respectively, and pump power is 5 W. The results suggest that a Pr^{3+}-doped chalcogenide fiber laser could efficiently lase within the range of 4.15–4.6 µm at fiber loss 1dB/m and 4.17–4.55 µm at fiber loss 3dB/m.

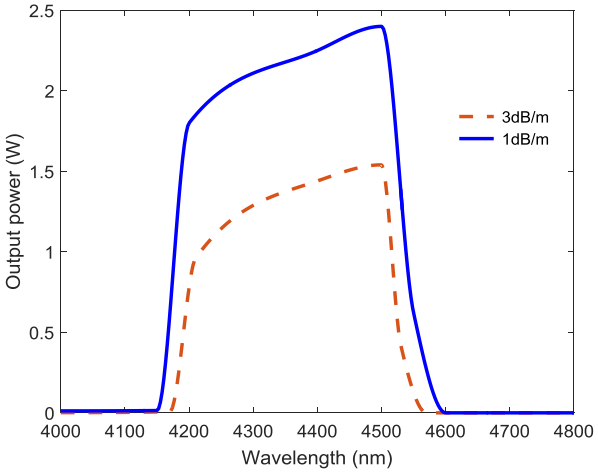

Fig. 8. Calculated output power as a function of lasing wavelength at a pump power of 5 W. The pump wavelength and fiber length are fixed at 2.04 µm and 1.3 m, respectively. Results are plotted for a fiber with a background loss of 1 dB⁄m and 3 dB⁄m, respectively.

IV. Conclusion

In this letter, we propose a highly efficient fiber laser design. The proposed layout avoids fabrication difficulties of cascaded FBGs in Pr^{3+}-doped chalcogenide glass fibers. The slope efficiency is more than three times higher when compared to a conventional cascade approach. Pr^{3+} ions have overlapping emission cross-sections in the ($^3F_2$, $^3H_6$) → $^3H_5$ (3.3–4.7 µm), and $^3H_5$→$^3H_4$ (3.7–5.5 µm) transitions. Exploiting this characteristic, the proposed design uses only one pair of FBG for idler and signal. Hence, it is avoiding the fabrication complexity which is related to the construction of two pairs of Bragg gratings and two lasing cavities. In addition, one excited ion in this approach can emit two photons in MID IR wavelengths as the same process in cross-relaxation transition of Tm^{3+} doped fiber laser and so increase the slope efficiency.

The simulation results reveal that more than 48% of slope efficiency could be achieved at wavelength 4.5µm and fiber loss of 1dB/m which is almost three times higher than conventional cascade pumping scheme. Moreover, the results suggest that a Pr^{3+}-doped chalcogenide fiber laser could efficiently laser within the range of 4.15–4.6 µm at fiber loss of 1dB/m and 4.17–4.55 µm at fiber loss of 3dB/m.

References

[1] H. Jelínková, O. Kőhler, M. Němec, P. Koranda, J. Šulc, V. Kubeček, P. Drlík, M. Miyagi, Y.-W. Shi, Y. Matsuura, M. R. Kokta, P. Hrabal, and M. Jelinek, "Comparison of mid infrared lasers effect on ureter tissue," *Laser Phys. Lett.*, vol.1, no.3, pp.143–146, 2004.

[2] F. Starecki *et al.*, "Mid-IR optical sensor for CO2 detection based on fluorescence absorbance of Dy^{3+}: Ga5Ge20Sb10S65 fibers," *Sens. Actuator B, Chem.*, vol. 207, no. 5, pp.518–525, Sep. 2015.

[3] M.L. Anne et al.," Fiber evanescent wave spectroscopy using the mid-infrared provides useful fingerprints for metabolic profiling in humans," *J. Biomed. Opt.*, vol.14, no.5, pp.054033-054033-9, 2009.

[4] M. C. Falconi *et al.*, "Dysprosium-Doped Chalcogenide Master Oscillator Power Amplifier (MOPA) for Mid-IR Emission," in *J. of Lightwave Tech.*, vol. 35, no. 2, pp.265-273, 2017.

[5] L. B. Shaw, B. Cole, P. A. Thielen, J. S. Sanghera, and I. D. Aggarwal, "Mid-wave IR and long-wave IR laser potential of rare-earth doped chalcogenide glass fiber," *IEEE J. of Quantum Electron*, vol.37, no.9, pp.1127–1137, 2001.

[6] R. G. DeCorby et al., "High-index-contrast waveguides in chalcogenide glass and polymer," *IEEE J. Sel. Top. Quantum Electron*, vol.11, no.2, pp.539-546, 2005.

[7] C R. Petersen, et al., "Mid-infrared supercontinuum covering the 1.4–13.3 µm molecular fingerprint region using ultra-high NA chalcogenide step-index fibre" *Nature Photonics*, vol.8, pp.830–834, 2014.

[8] G. E. Snopatin, V. S. Shiryaev, V. G. Plotnichenko, E. M. Dianov, and M. F. Churbanov, "High-purity chalcogenide glasses for fiber optics," *Inorg Mater*, vol.45, no.13, pp.1439–1460, 2009.

[9] Ł. Sójka, Z. Tang, H. Zhu, E. Bereś-Pawlik, D. Furniss, A. B. Seddon, T. M. Benson, and S. Sujecki, "Study of mid-infrared laser action in chalcogenide rare earth doped glass with Dy^{3+}, $Pr^{3+}$and Tb^{3+}," *Opt. Mater. Express*, vol.2, pp.1632-1640, 2012.

[10] R Chahal, et al., "Fiber evanescent wave spectroscopy based on IR fluorescent chalcogenide fibers," *Sensors and Actuators B: Chemical* vol.229, no.28, pp.209–216, 2016.

[11] J. Hu, C. R. Menyuk, C. Wei, L. B. Shaw, J. S. Sanghera, and I. D. Aggarwal, "Highly efficient cascaded amplification using Pr^{3+}-doped mid-infrared chalcogenide fiber amplifiers," *Opt. Lett.*, vol.40, pp.3687-3690, 2015.

[12] M. C. Falconi, G. Palma, F. Starecki, V. Nazabal, J. Troles, S. Taccheo, M. Ferrari, and F. Prudenzano, "Design of an Efficient Pumping Scheme for Mid-IR Dy^{3+}: Ga5Ge20Sb10S65 PCF Fiber Laser," *IEEE Photon. Technol. Lett.*, vol.28, no.18, pp.1984–1987, Sep. 2016.

[13] S. Sujecki, "An Efficient Algorithm for Steady State Analysis of Fibre Lasers Operating under Cascade Pumping Scheme," *International Journal of Electronics and Telecommunications*, vol.60, no.2, PP.143-149, 2014.

[14] R. S. Quimby, L. B. Shaw, J. S. Sanghera and I. D. Aggarwal, "Modeling of Cascade Lasing in Dy: Chalcogenide Glass Fiber Laser with Efficient Output at 4.5 µm," in *IEEE Photonics Technology Letters*, vol. 20, no. 2, pp. 123-125, Jan.15, 2008.

[15] P F. Moulton, et al., "Tm-Doped Fiber Lasers: Fundamentals and Power Scaling" *IEEE J. Sel. Top. Quantum Electron*, vol.15, no.1, pp.85-92, Jan. 2009.

[16] S. Sujecki et al., "Theoretical study of population inversion in active doped MIR chalcogenide glass fibre lasers (invited)", *Opt. Quant Electron*, vol.47, no.6, pp. 1389–1395, 2015.

[17] S. Sujecki *et al.*, "Modelling of chalcogenide glass fibre lasers for MIR generation," *2012 14th International Conference on Transparent Optical Networks (ICTON)*, Coventry, pp.1-5, 2012.